

## Development of High-Power Rectifier for Power Factor Correction Using Interleaved Boost Topology

Prakash Kharade<sup>1\*</sup>, Mahadev D Uplane<sup>2</sup>

<sup>1</sup>Department of Technology, Shivaji University, Kolhapur 416004, India

<sup>2</sup>Department of Instrumentation Science, SP Pune University, Ganeshkhind, Pune 411007, India

\*Correspondence to: Prakash Kharade, Department of Technology, Shivaji University, Kolhapur 416004, India, Tel 9594649029; E-mail: kharadepa@yahoo.co.in

Received date: August, 20, 2021; Accepted date: November 17, 2021; Published date: November 26, 2021

Citation: Kharade P, Uplane MD (2021) Development of High-Power Rectifier for Power Factor Correction Using Interleaved Boost Topology. J Electr Eng Electron Technol 10: 11.

### Abstract

In this paper, a 2KW rectifier with power factor correction is designed and developed. The converter is applied for server application, which adopts two phase interleaved boost converter (IBC). The circuit operates in continuous current conduction (CCM) mode and use a cascade control strategy. Cascade control has two loops; inner current loop uses average current control and outer voltage loop uses PI control strategy. In order to verify feasibility of proposed scheme, firstly; a 2KW IBC type PFC is simulated using PSIM software and then a prototype is developed which is converting 180-260V AC input voltage to 400V DC output voltage, is implemented using a Microchip IC dsPIC33FJ16GS504. The experimental results are satisfactory, which reveal that a power factor is 0.9992 (close to unity), THD less than 5% and more than 98% efficiency at 100 KHz switching frequency, 230Vrms input voltage and power output from 400W to 2KW.

**Keywords:** Two Faze interleaved boost converter; CCM; power factor correction; PI control; wide voltage input range; 16 bit micro-controller

### Introduction

In the present time, greater part of the electronic gadgets use DC supply. Transformation of AC to DC is comprehensively used in various applications, for example, Switched Mode Power Supplies, battery chargers, power supplies to communication systems, washing machines, air-conditioners, servers, and so on. Because of presence of diodes, ordinary rectifiers followed by substantial size capacitors for energy storage, acts as a nonlinear load to power line and the power factor of such circuits is very low, even lower than 0.7. Ordinary rectifiers have irregular and non-sinusoidal line currents injecting large amount of harmonics in line and polluting the power supplies. These low order line current harmonics distorts the voltage at common coupling. In addition to voltage distortions, it also increases current ratings of line, due to large currents; heating of the equipment's, low

efficiency, large size line filtering requirement are some of the drawbacks. Therefore to avoid all these consequences and to improve power quality as per the international standards an appropriate power factor corrector must be used [1].

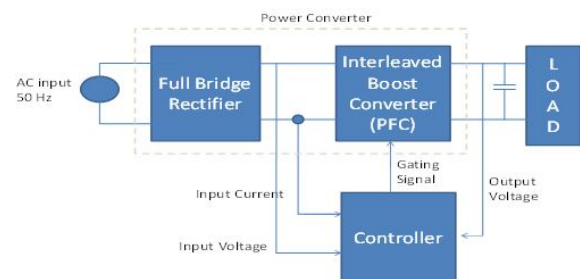
Numbers of active and passive circuits were utilized by numerous specialists to address this issue [3], [12]. The most straightforward approach is to use passive PFCs which improves power factor to somewhat acceptable level. Out of the solutions available in literature, passive PFCs are effective for low power applications most extreme up-to 200W. Disadvantages of passive PFCs are enormous in size, critical reliance of average output voltage on load change and are more expensive. To resolve this issue active PFCs were suggested by many researchers [4].

In this paper, two main converter topologies, boost and interleaved boost are investigated and analyzed for enhancing PF, THD and efficiency in single phase power supply. Both topologies are operated at switching frequency 100 kHz with 2 kW output power and 400V output DC voltage to provide THDi less than 5%, efficiency greater than 95% and PF close to unity [2].

The paper is structured in the following manner: The control strategy for both a boost and interleaved boost converter is presented in the second section. Afterward, in third section the design of the converter system with average current control is explained. The fourth section is dedicated to present the results of simulation using PSIM software. The fifth section shows the experimental results and explains micro-controller-based implementation of real-time model. Finally, conclusions are conferred in the last section.

The block diagram of interleaved PFC converter based on average current control is shown in Fig.1. Power converter uses a diode rectifier followed by a bulk capacitor to convert AC voltage to DC voltage, followed by an interleaved boost converter which acts as an active PF corrector. For controlling the output voltage and correcting the input power factor, the dc output voltage, input ac current and input ac voltage are given as a feedback signals to the controller. Controller has its own reference levels and according to the error it manipulates the actuating signals and provides the gate signals to the active device MOSFETs to control the output voltage and input power factor.

**Figure1:** Block Diagram of 2KW PFC Interleaved Boost Converter and its control.

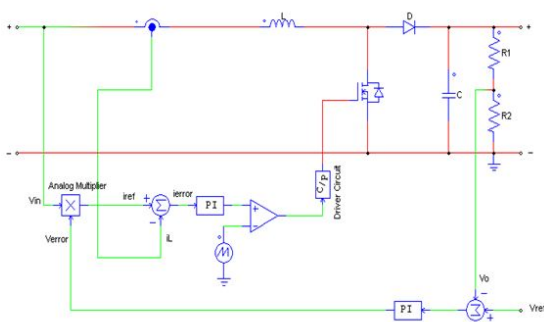


Proposed Interleaved Boost Topology and Control Strategy

**PFC by Average Current Control using Boost Topology:**

There are distinctive current mode control techniques like variable frequency Peak current control, Hysteresis control, and average current control. Out of which average current control demonstrates better outcomes. It is more desired than other control strategies because line current can be approximated by the average of current per switching cycle [7]. The fundamental circuit diagram of Boost converter is shown in Fig.2. For regulation of output voltage and simultaneously correction of power factor here cascade control is utilized. There are two loops in cascade control: inner loop and outer loop. Outer voltage loop maintains the output voltage to a set value and inner current loop does the job for power factor correction by continuously comparing input current  $I_L$  with reference current  $I_{ref}$ . By utilizing PI controller alongside PWM technique, gate signals are generated which controls on time i.e., duty cycle of the active switching device.

**Figure 2:** Average current control strategy for boost converter.



**PFC by Average Current Control using Interleaved Boost Topology:**

In conventional boost topology, volume of inductor is substantially large, and ripple current cancellation is not possible. These limitations can be overwhelmed by utilization of interleaved boost converter (IBC). IBC comprises of two boost converters connected in parallel, operating at  $180^\circ$  phase shift. The input current is the addition of two inductor currents. As the ripple currents streaming in two inductors are out of phase, they tend to cancel each other and so total harmonics in the input side is decreased. At 50% duty cycle, cancellation of ripple current is the most ideal.

Capacitor current in the output is the sum of two diode currents ( $I_{D1}$  and  $I_{D2}$ ) minus the load current ( $I_L$ ).  $F_s$  is the switching frequency,  $T_s$  is the time-period of one switching cycle and  $D$  is the Duty cycle. During the  $D \cdot T_s$  period, switch  $S_1$  is ON and inductor current  $I_L$  flows to energize the inductor. During the period  $(1-D) \cdot T_s$  of the switching cycle,  $S_1$  is OFF but inductor current cannot change instantly. The inductor current starts decreasing. This change in current  $di/dt$  creates adequate voltage ( $L \cdot di/dt$ ) across the inductor with a polarity such as to drive current through diode  $D_1$  to charge the output capacitor [6].

A fundamental boost PFC converter converts a DC voltage to a larger DC level. The interleaved boost PFC increases the voltage level, however as it comprises of two boost converters in parallel so includes the advantage of two phases activated at 180 degrees out of stage [7]. Conduction losses in the switches and diodes can be decreased by partitioning the current into two power paths, which finally results in gain of overall efficiency compared to a boost converter. As effective ripple frequency at output is doubled, making ripple voltage reduction

much easier, hence the power loss in overall circuit is reduced [10]. The circuit diagram of IBC converter is shown in Fig.3a.  $V_{in}$  the source input voltage,  $V_{L1}$  and  $V_{L2}$  are the voltages across  $L_1$  and  $L_2$  respectively.  $I_{L1}$ ,  $I_{L2}$  are the currents flowing through inductor  $L_1$  and  $L_2$  respectively.  $I_c$  and  $I_o$  are currents flowing through output capacitor and load. Modes of operation of the interleaved boost topology are shown in Fig.3.

In mode1 appeared in Fig.3b, switches  $S_1$  and  $S_2$  are ON, diodes  $D_1$  and  $D_2$  are OFF, current through  $L_1$  and  $L_2$  increases depending on input voltage and stores the energy in  $L_1$  and  $L_2$ . The sum of  $V_{L1}$  and  $V_{L2}$  during this time is  $V_{in}$ . A inductor current increments linearly with the slope of  $V_{in}/2L$ . During this time the current through  $S_1$  and  $S_2$  is same as  $I_{L1}$  and  $I_{L2}$  respectively. In mode 2,  $S_2$  turns OFF,  $D_2$  turns ON as the input voltage becomes higher than the output voltage to deliver part of its stored energy to the load and output capacitor as shown in Fig.3c. The current in  $L_2$  inclines down with a slant subject to the contrast between the input and output voltage. Mode 3 is similar to Mode 2 here  $S_1$  turns off and  $D_1$  turns on as shown in Fig.3d. The current in  $L_1$  inclines down with a slope dependent on the difference between the input and output voltage in Mode 4 as shown in Fig.3 (e),  $S_1$  and  $S_2$  are off, both  $L_1$  and  $L_2$  deliver their part of energy to the load and the output capacitor, as a result current in  $L_1$  and  $L_2$  ramps down. For controlling of interleaved boost converter using PI average current control technique the sensing of output voltage, input currents and the input voltage is necessary [15]. An opto-coupler and potential transformer are used to sense the input voltage [5], [10]. An input current is detected by using current transformer or Hall- effect sensor. Here two boost converters are connected in parallel to share the total load as shown in interleaved boost converter. Each converter will deliver only the portion of the power that it is programmed for by its reference current limit [15].

**Figure 3:** Circuit configuration of a Interleaved Boost PFC converter: a) With operational switch: - b) Mode 1  $S_1$  and  $S_2$  ON, c) Mode 2  $S_1$  ON and  $S_2$  OFF, d) Mode 3  $S_1$  OFF and  $S_2$  ON , e) Mode 4  $S_1$  and  $S_2$  OFF.

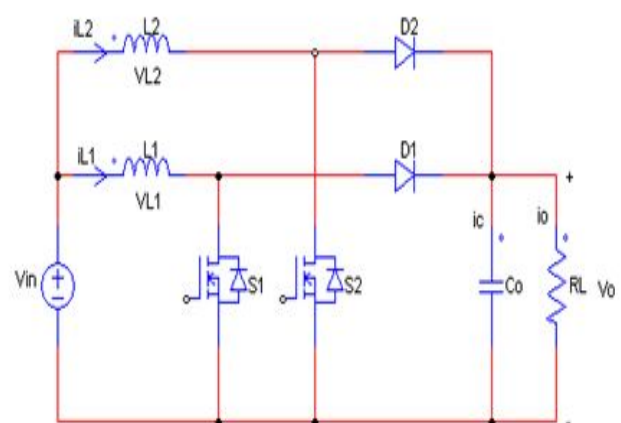


**Figure 3.a**

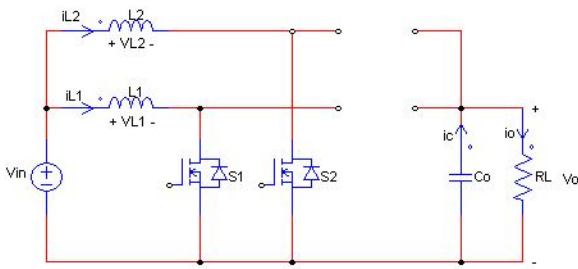


Figure 3.b Mode 1

$$\frac{di_{L1}}{dt} = \frac{V_{in}}{L_1}$$

$$\frac{di_{L2}}{dt} = \frac{V_{in}}{L_2}$$

$$\frac{dV_o}{dt} = \frac{-V_o}{RC}$$

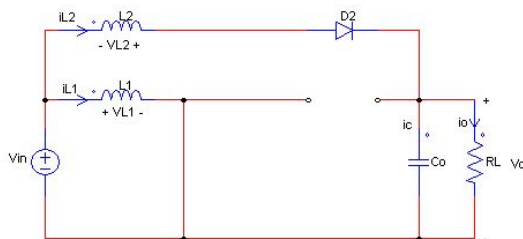


Figure 3.c Mode 2

$$\begin{bmatrix} \frac{di_{L1}}{dt} \\ \frac{di_{L2}}{dt} \\ \frac{dV_o}{dt} \end{bmatrix} = \begin{bmatrix} 0 & 0 & 0 \\ 0 & 0 & 0 \\ 0 & 0 & -\frac{1}{RC} \end{bmatrix} \begin{bmatrix} i_{L1} \\ i_{L2} \\ V_o \end{bmatrix} + \begin{bmatrix} \frac{1}{L_1} \\ \frac{1}{L_2} \\ 0 \end{bmatrix} V_{in} \quad (1)$$

Mode 2: Switches S1 diode D2 are ON, and S2 and D1 are OFF.

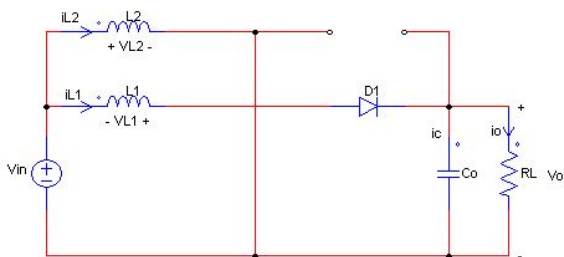


Figure 3.d Mode 3

$$\frac{di_{L1}}{dt} = \frac{V_{in}}{L_1}$$

$$\frac{di_{L2}}{dt} = \frac{V_{in}}{L_2} - \frac{V_o}{L_2}$$

$$\frac{dV_o}{dt} = \frac{i_{L2}}{C} - \frac{V_o}{RC}$$

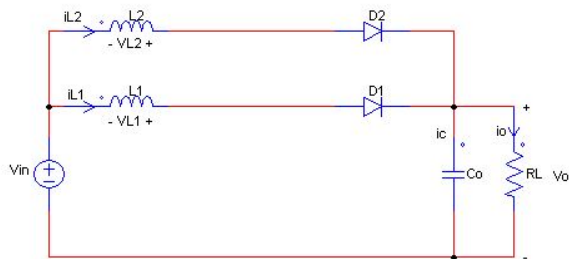


Figure 3.e Mode 4

$$\begin{bmatrix} \frac{di_{L1}}{dt} \\ \frac{di_{L2}}{dt} \\ \frac{dV_o}{dt} \end{bmatrix} = \begin{bmatrix} 0 & 0 & 0 \\ 0 & 0 & -\frac{1}{L_2} \\ 0 & \frac{1}{C} & -\frac{1}{RC} \end{bmatrix} \begin{bmatrix} i_{L1} \\ i_{L2} \\ V_o \end{bmatrix} + \begin{bmatrix} \frac{1}{L_1} \\ \frac{1}{L_2} \\ 0 \end{bmatrix} V_{in} \quad (2)$$

The inductor currents  $i_{L1}$  and  $i_{L2}$  with the output capacitor voltage  $V_o$  are assumed as state variables. The converter comprises of four modes of operation.

**Mode1** : Switches S1 and S2 are ON, diode D1 and D2 are OFF. At this stage, the state differential equations of the circuit are given by:

**Mode 3:** Switch S2 and diode D1 are ON, and Switch S1 and diode D2 are OFF.

$$\begin{aligned} \frac{di_{L1}}{dt} &= \frac{V_{in}}{L_1} - \frac{V_o}{L_1} \\ \frac{di_{L2}}{dt} &= \frac{V_{in}}{L_2} \\ \frac{dV_o}{dt} &= \frac{i_{L1}}{C} - \frac{V_R}{RC} \end{aligned}$$

$$\begin{bmatrix} \frac{di_{L1}}{dt} \\ \frac{di_{L2}}{dt} \\ \frac{dV_o}{dt} \end{bmatrix} = \begin{bmatrix} 0 & 0 & -\frac{1}{L_1} \\ 0 & 0 & 0 \\ \frac{1}{C} & 0 & -\frac{1}{RC} \end{bmatrix} \begin{bmatrix} i_{L1} \\ i_{L2} \\ V_o \end{bmatrix} + \begin{bmatrix} \frac{1}{L_1} \\ \frac{1}{L_2} \\ 0 \end{bmatrix} V_{in} \quad (3)$$

**Mode 4:** Switches S1 and S2 are OFF, diode D1 and D2 are ON.

$$\begin{aligned} \frac{di_{L1}}{dt} &= \frac{V_{in}}{L_1} - \frac{V_o}{L_1} \\ \frac{di_{L2}}{dt} &= \frac{V_{in}}{L_2} - \frac{V_o}{L_2} \\ \frac{dV_o}{dt} &= \frac{i_{L1}}{C} + \frac{i_{L2}}{C} - \frac{V_R}{RC} \end{aligned}$$

$$\begin{bmatrix} \frac{di_{L1}}{dt} \\ \frac{di_{L2}}{dt} \\ \frac{dV_o}{dt} \end{bmatrix} = \begin{bmatrix} 0 & 0 & -\frac{1}{L_1} \\ 0 & 0 & -\frac{1}{L_2} \\ \frac{1}{C} & \frac{1}{C} & -\frac{1}{RC} \end{bmatrix} \begin{bmatrix} i_{L1} \\ i_{L2} \\ V_o \end{bmatrix} + \begin{bmatrix} \frac{1}{L_1} \\ \frac{1}{L_2} \\ 0 \end{bmatrix} V_{in} \quad (4)$$

Design Parameters For Proposed Topology

The key circuit parameters and specifications are listed as below:

$$V_{in}(t) = 180V \sim 260V,$$

$$V_o = 400VDC \pm 1\%$$

$$P_o = 2000W, F_s = 100kHz$$

$$L_{in} = 520\mu H \text{ for Boost, } L_1 = 520\mu H, L_2 = 520\mu H \text{ for IBC,}$$

$$C_o = 1410\mu F$$

where  $V_{in}(t)$  is the AC RMS input voltage,  $V_o$  is the regulated output dc voltage,  $P_o$  is the output power,  $F_s$  is the switching frequency,  $L_{in}$  is the boost inductance,  $C_o$  is the output capacitance.

### Design for Boost Inductor

The design of boost inductor is a critical part. The inductor determines amount of ripple current in the input current. The inductor is to be designed at the minimum input voltage of circuit [7]. At full load current, and when the input voltage is minimum; the maximum

current flows through inductor, the corresponding maximum duty cycle is given by:

$$d = [V_o - \sqrt{2} * V_{in(\text{min pk})}] / V_o \quad \dots (5)$$

And, boost inductor is calculated by:

$$L_1, L_2 = [V_{in(\text{min pk})} * d * T_s] / \Delta i \quad \dots (6)$$

Where,  $V_{in(\text{min pk})}$  is the minimum peak input voltage,  $V_o$  is output voltage,  $d$  is maximum duty ratio,

$T_s$  are the time period of one switching cycle, and  $\Delta i$  is allowed ripple current in percentage [9].

### Design for Output Capacitor

The output capacitor for PFC pre-regulator is selected as per the requirement of hold-up time. Hold up time is the function of energy storage capacity of the capacitor, load power and the minimum and maximum limits of the output voltage.

The value of  $C_{min}$  is given by:

$$C_o = [2 * P_{out} * t_h] / [(V_{o(\text{max})}^2 - (V_{o(\text{min})}^2)] \quad \dots (7)$$

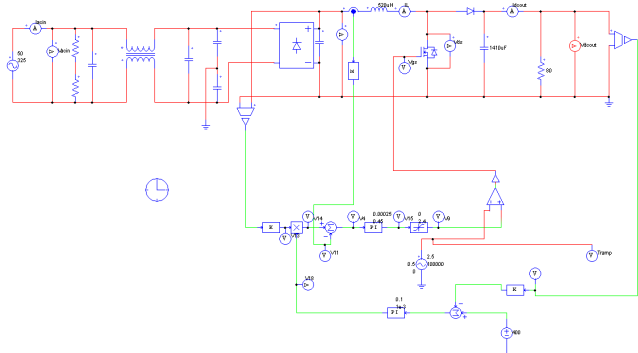
Where,  $P_{out}$  is the maximum output power,  $t_h$  is the hold-up time,  $V_{o(\text{max})}$  is the maximum output voltage and  $V_{o(\text{min})}$  is the minimum output voltage.

### Controller Design

#### Control Strategy of Average Current Mode for Conventional BOOST topology:

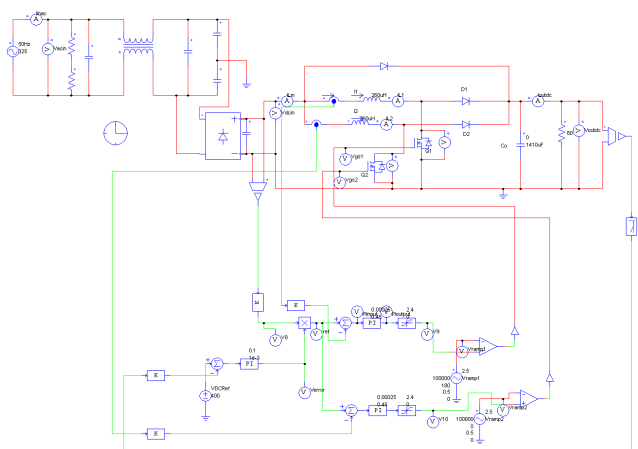
Control technique with Average Current Mode for conventional boost converter is shown in Fig. 4. The current passing through inductor  $L$  ( $i_L$ ) is compared with the reference current ( $i_{ref}$ ), and is processed using current error amplifier. Then, the average error current, is amplified, compared with the triangular wave, and which provides the PWM drive signal for the switching transistor. When the inductor current  $i_L$  increases, the error current  $I$  error decreases, the output duty cycle for PWM comparator decreases, results in reduced inductor current  $i_L$ . In contrast, the inductor current  $i_L$  increases. When the desired output voltage  $V_o$  increases, the output of comparator decreases, so error current  $I$  error decreases, the output duty cycle for PWM comparator decreases, results in less inductor current  $i_L$  and output voltage  $V_o$ . In contrast, the output voltage  $V_o$  increases.

**Figure 4:** Simulation Circuit of Average current control strategy for Boost converter Control Strategy of Average Current Mode for Interleaved BOOST topology:



In high power applications, to overcome the limitations of the boost converter, interleaved boost converter is a better choice. The IBC takes advantage of ripple reduction and input power sharing between the different converters connected in parallel. Due to the distribution of input power and low circulating harmonic currents, the magnetic volume is greatly reduced [13]. In addition, as ripple content in the output is less which avoids additional output filter requirement [12]. Fig.5 shows the interleaved boost converter with two boost phases triggered with a phase shift of 180°. A few disadvantages of this topology are the number of components, implementation cost is moderate and little more control complexity, as presented by [3], [4].

**Figure 5:** Simulation Circuit of Average current control strategy for Interleaved Boost Converter.



**Simulation results**

A 2000W model is simulated using PSIM software to assess Boost converter and Interleaved Boost converter with PI average current control strategy. The Input AC RMS voltage is 230 V and the output DC voltage is 400V. The AC input voltage-current waveforms and DC output voltage-current waveforms of boost converter and interleaved boost converter are shown in Fig. 6a and Fig. 6b, respectively. And the Fast Fourier Transform (FFT) of ripple current in boost converter and interleaved boost converter are shown in Fig. 7a and Fig. 7b, respectively. The rectified AC input is boosted using Boost and Interleaved boost converter. For closed loop operation in real time implementation input voltage, inductor current and output voltage will be sensed using current transformer and potential transformer. The converters are operated at 100 kHz switching frequency, 2000W output power with the reference voltage of 400V.

**Table I:** PSIM Simulation Results of Boost Converter Pout=2000Watts L = 520uH, Co = 1410uF.

Sr. No	Vin AC Vrms	Iin AC (A)	Pin (W)	RL (Ω)	Vout DC (V)	Iout DC (A)	Pout (W)	P.F.	THD %	Effi %
1	230	12.56	2021	80	400.39	5.00	1998	0.9949	8.44	98.86
2	230	9.97	1616	100	400.44	4.00	1597	0.9935	8.80	98.22
3	230	7.42	1228	133	400.37	3.00	1201	0.9912	9.17	97.80
4	230	4.92	822	200	400.00	2.00	798	0.9862	10.30	97.10
5	230	3.31	5610	300	399.30	1.33	530	0.9791	12.30	94.46
6	230	2.47	4340	400	397.32	0.99	393	0.9735	15.20	90.58

**Table II:** PSIM Simulation Results of IBC Interleaved Boost Converter Pout= 2000Watts L1 =L2= 520μH, Co = 1410μF.

Sr. No	Vin AC Vrms	Iin AC (A)	Pin (W)	RL (Ω)	Vout DC (V)	Iout DC (A)	Pout (W)	P.F.	THD %	Effi %
1	230	12.77	2032	80	399.41	4.99	1996	0.9993	3.46	99.46
2	230	10.18	1630	100	399.29	3.99	1593	0.9984	4.62	98.72
3	230	7.73	1233	133	398.21	2.99	1192	0.9965	6.12	96.63
4	230	5.25	845	200	393.68	1.97	775	0.9917	9.97	91.75
5	230	3.52	5680	300	398.66	1.32	530	0.9815	11.9	93.05
6	230	2.97	4270	400	400.00	1.00	399	0.9812	16.3	93.5

**Figure 6a:** Input-Output Waveforms of Boost Converter.

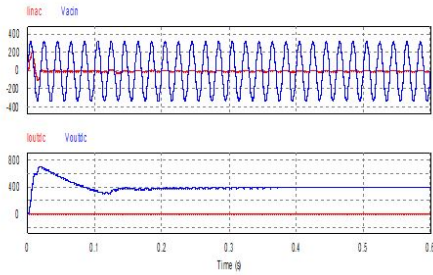


Figure 6b: Input-Output Waveforms of IBC Converter.

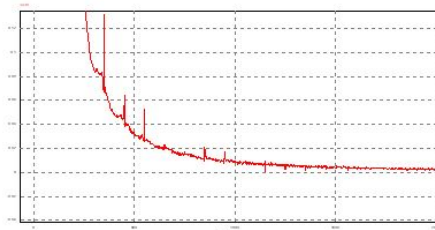


Figure 7a: Fast Fourier Transform of ripple current in Boost Converter.

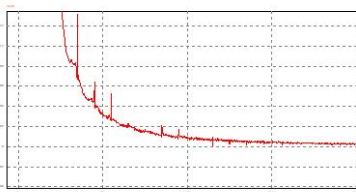


Figure 7b: Fast Fourier Transform of ripple current in Interleaved Boost Converter.

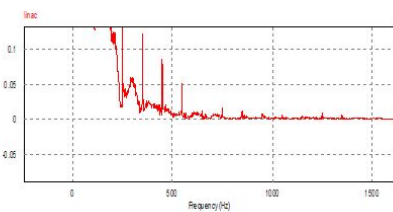


Figure 8a: THD versus Output Power for Boost and IBC.

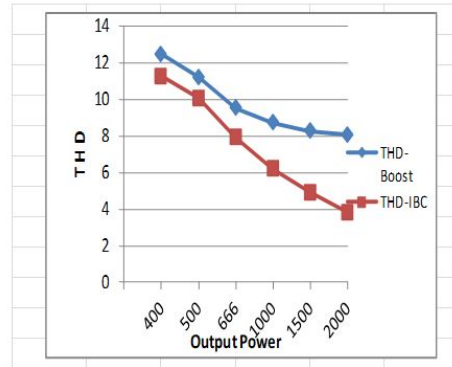


Figure 8b: PF versus Output Power for Boost and IBC.

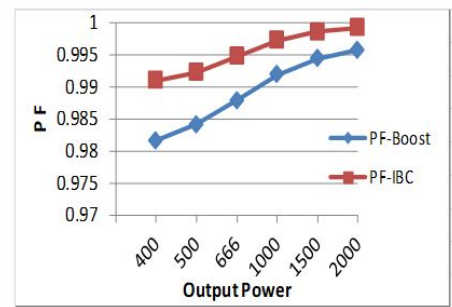


Figure 8c: Efficiency versus Output Power for Boost and IBC.

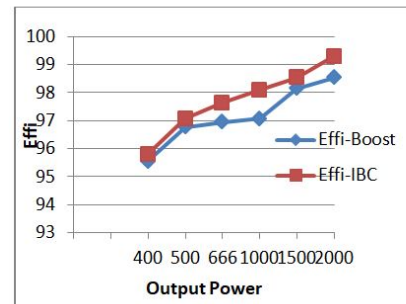


Table III: Comparative Performance of PSIM Simulated Results.

Topology	P.F.	T.H.D. %	Efficiency %
Boost	0.9949	8.44	98.86
IBC	0.9993	3.46	99.46

The comparative Simulation performance of conventional Boost, and Interleaved Boost Converters (IBC) based PFC is shown in Table III for 230Vrms AC input at 100 kHz switching frequency, 2KW output power and 400V dc output voltage. Fig.8a, Fig.8b and Fig.8c shows THD, PF and overall efficiency comparison of boost and IBC topology, respectively. Simulation results reveal that, the overall efficiency of the IBC type converter has improved i.e., 99.46% compared to boost type converter. The THD has been reduced to

3.46% which is as per the IEC61000-3-2 Standards and there is an improvement in power factor 0.9993.

As exhibited through this paper, interleaving boost type rectifiers provide high frequency input current ripple cancellation. Because of decreasing amplitudes of the input current ripple, there is a decrease in filter size. A comparison of boost and interleaved boost type PFC revealed that the interleaving is a extremely successful technique for lessening input line current harmonics.

### Experimental results

An experimental prototype of high-power rectifier based on average current control with IBC topology, which is controlled by dsPIC33fj16gs504, is developed to confirm the operational working of the proposed converter. Fig.9 shows the experimental prototype for proposed 2KW Interleaved Boost PFC converter. Components and devices used are recorded in Table IV.

**Table IV:** Devices and Components used for Experimental Model.

Parameter	Manufacturer	Value
CoolMOS MOSFETs	Infineon Technologies	SPI20N60C3
Boost Diodes	IXYS	DSEI60-12A
Full-Bridge Rectifier	International Rectifier	GBU25J
Boost Inductor	Neha Tech Services	550µH
Output Capacitor	ALCON Electronics	2200µF
Load Resistor	-	80-400Ω
Current Sensor	Neha Tech Services	Current Transformer CT
Voltage Sensor	-	Potential Divider

### Prototype

Figure 9 demonstrates the picture of hardware model: the power circuit, control card and auxiliary power supply. The power circuit contains the high power converter and the regulated auxiliary power supplies for the control circuit. The control PCB contains the signal conditioning circuits and the micro-controller. The power stage is the well-known circuit and; hence, we mention only the characteristics of control circuit.

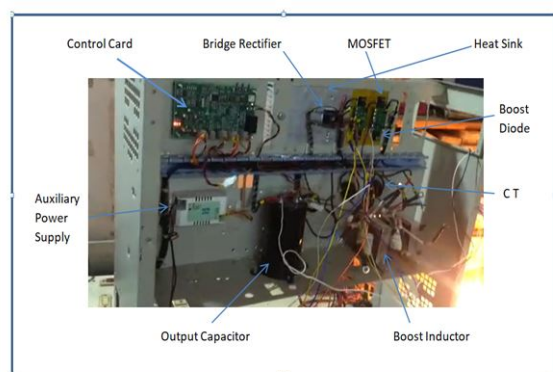
A 16-bit micro-controller dsPIC33FJ16GS504 from Microchip technologies is used for controlling the converter. The micro-controller operates with clock frequency of 40 MHz. We have used five ADCs simultaneously operating at same sampling rate.

The input current sensed by Shunt resistance is amplified by differential amplifier and fed to the analog channel of the ADC (0 - 3.3v).

The sensed output voltage is conditioned by a potential divider and to minimize the ripple current in the output it is filtered by a low-pass filter with cut off frequency of 88Hz.

A +12V auxiliary power supply is necessary to feed the gate drive circuit. To feed the micro-controller an auxiliary source of 5V has been used. The gating signals for MOSFETs are generated with a driver circuit IC MCP1403 of Microchip Technologies.

**Figure 9:** Pictures of the Experimental Model: a) Power Circuit, b) Control Card, c) Auxiliary Power Supply.



### Algorithm

The control algorithm functions with internal timer interruption which is defined to be of a sample time 50µs. In inner current control loop for the purpose of data acquisition and AtoD conversion it needs 27µs. The difference equation of voltage controller is segmented to distribute the computational charge cycle-by-cycle. Hence, the total sample time does not surge substantially, and the sample time required for the outer control loop can be defined easily. We have defined the sample time of 500µs for the outer voltage control loop.

**Table VI:** Results of Hardware implemented IBC Interleaved Boost type high power Converter L1 =L2= 550µH, Co = 2200µF.

Sr. No	V <sub>in</sub> (V <sub>rms</sub> )	I <sub>in</sub> (A)	P <sub>in</sub> (W)	R <sub>L</sub> (Ω)	V <sub>out</sub> (V)	I <sub>out</sub> (A)	P <sub>out</sub> (W)	P.F.	THD %	Eff %
1	230	13.50	2030	80	399.50	4.98	1990	0.9992	4.11	98.00
2	230	11.00	1630	10	399.20	3.94	1575	0.9980	4.82	96.62
3	230	8.50	1152	15	398.10	2.76	1100	0.9930	6.38	95.48
4	230	6.50	745	20	393.20	1.75	700	0.9810	9.00	93.95
5	230	4.00	525	30	398.50	1.23	490	0.9800	12.15	93.33
6	230	3.00	400	40	400	0.923	368	0.9780	17.3	92.00

**Figure10a:** THD versus Output Power for Prototype IBC.

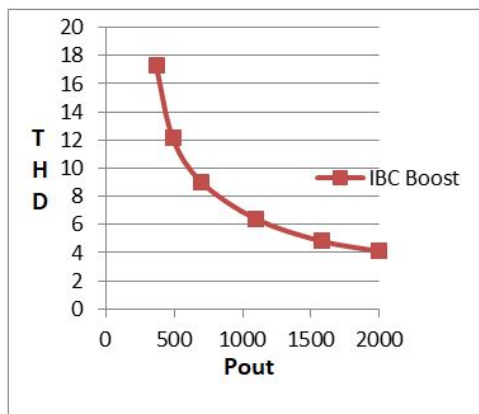


Figure 10b: PF versus Output Power for Prototype IBC.

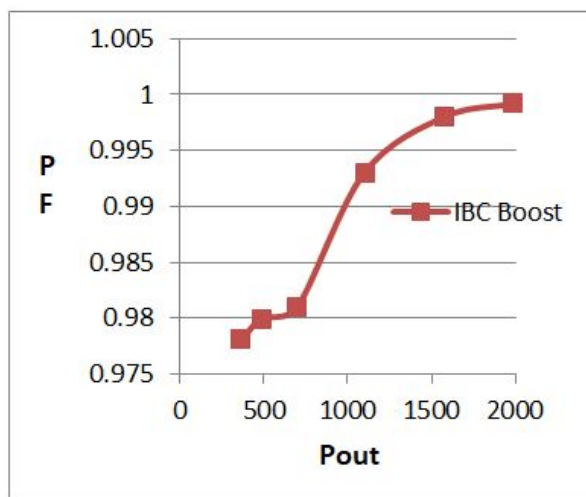
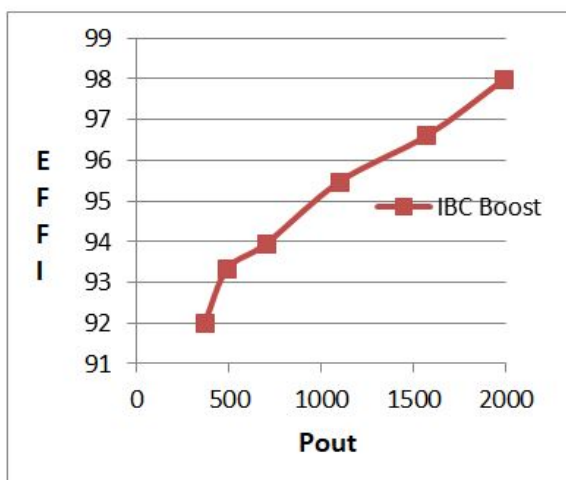


Figure 10c: Efficiency versus Output Power for Prototype IBC.



## Results and Discussion

Table VII: Comparative Analysis of PF, THD and Efficiency of Proposed Converter.

Topology	P.F.	T.H.D. %	Efficiency %
Boost Simulation	0.9949	8.44	98.86
IBC Simulation	0.9993	3.46	99.46
IBC Prototype	0.9992	4.11	98.00

PSIM Simulation results for IBC type PFC converter are shown in Fig.9a, Fig.9b and Fig.9c. Results obtained from experimental model are presented in Fig.10a, Fig.10b and Fig.10c, respectively.

The proposed 2KW IBCPFC Converter which is having two-phase interleaved boost PFC have the subsequent features:

As in IBC two boost topologies are switching at 180 degree, i. e. out of phase, their inductor currents are also staggered and cancel with each other; so effective ripple in input current is reduced. So THD is reduced. As switches are operated at high frequency, and ripple current is twice for each phase, which reduces required size of EMI filter. As high-frequency ripple current in the output capacitor is reduced, so required value of output capacitor declines. Finally, input line current wave tracks better the input voltage wave, so the power factor is very high.

## Conclusion

In this work, a front-end 2KW interleaved boost type PFC converter for power factor correction is proposed using PI controller in CCM mode. The feasibility and reliability of the proposed converter is first verified by simulation in PSIM software and then confirmed by a hardware prototype model. As per simulation results, the conventional boost converter has overall efficiency of 98.86% and THDi = 8.44%, PF 0.9949 and the interleaved boost converter has efficiency of 99.46 % and THDi = 3.46%, PF = 0.9993. Simulation results are confirmed by the hardware prototype implementation of the developed converter. According to results of implemented model, the overall efficiency is 98.00%, THDi is = 4.11% and PF is = 0.9992. At last, the THD measured on prototype model is in great agreement with the results obtained by simulation and is fit in with IEEE and IEC standards.

## References

- [2] Supratim Basu, and Math H.J. Bollen, Tore M. (2004) Undeland, "PFC strategies in light of EN 61000-3-2," Presented at EPE PEMC 2004 conference at Riga, Latvia, 1-3.
- [3] Oscar Gracia, Jose A. Cobos, Roberto Prieto and Javier Uceda (2003) "Single- Phase Power Factor Correction: A Survey," IEEE Transactions on Power Electronics, Vol. 18, No3, pp-749-755.
- [4] Bhim Singh, Sanjeev Singh, Ambrish Chandra, Kamal Al-Haddad (2011) "Comprehensive Study of Single-Phase AC-DC Power Factor Corrected Converter with High-Frequency Isolation," IEEE Transactions on Industrial Informatics, vol.7, No.4, pp 540-556.
- [5] L.Umanand (2013) "Power Electronics Essentials and Applications," Wiley India Pvt. Ltd, pp 201-213



5. [6] P.A. Kharade, Dr. M.D. Uplane (2020) "Performance Analysis of High Power PF Corrector by Co-Simulation using PSIM and MATLAB/Simulink," *Int J Sci Tech Res*, Vol.9 Issue 1, pp 4688-4694.
6. [7] B. A. Miwa, D. M. Otten, M. E. Schlecht (1992) "High Efficiency Power Factor Correction Using Interleaving Techniques," proceeding of APEC'92, Applied Power Electronics Conference and Exposition, pp: 557 – 568
7. [8] T. Nussbaumer, K. Raggl, and J. W. Kolar (2009) "Design guidelines for interleaved single-phase boost PFC circuits," *IEEE Trans. Ind. Electron.*, vol. 56, no. 7, pp. 2559–2573, Jul.
8. [9] M.Rashid (2001) "Power Electronics Handbook," 2nd Edition, Prentice Hall, pp 167- 185.
9. [10] J. Liu, W. Chen, J. Zhang, D. Xu, and F.C. Lee (2001) "Evaluation of power losses in different CCM mode single-phase boost PFC converters via simulation tool," *IEEE Industry Applications Conf. (IAS) Record*, Session: High frequency power conversion, Paper 4.
10. [11] A. Pandey, B. Singh, D. P. Kothari (2004) "Comparative Evaluation of Single-phase Unity Power Factor ac-dc Boost Converter Topologies," proceeding of *IE (I) Journal-EL*, pp 102-109, vol 85.
11. [12] L. Rossetto, S. Buso and G. Spiazzi (2000) "Conducted EMI Issues in a 600-W Single Phase Boost PFC Design," *IEEE Transactions on Industry Applications*, Vol. 36, No. 2
12. [13] Burak Akin (2012) "Comparison of Conventional and Interleaved PFC Boost Converters for Fast and Efficient Charge of Li-ion Batteries Used in Electrical Cars," 2012 International Conference on Power and Energy Systems Lecture Notes in Information Technology, Vol.13.
13. [14] M.ArunDevi, K.Valarmathi, R. Mahendran (2014) "Ripple Current Reduction in Interleaved Boost converter by Using Advanced PWM Techniques," *IEEE International Conference on Advanced Communication Control and Computing Technologies (ICACCCT)*.
14. [15] P.A.Kharade, R.Rashmi, M.D.Uplane (2017) "P F Improvement in Single- Phase High Power Rectifiers with Interleaved Boost Topology," *IEEE International Conference on Power, Control, Signals and Instrumentation Engineering, ICPCSI, Chennai, India. Issue I*, pp 153-159.
15. [16] LU Xiang, XIE YUN-xiang, LI Quang-jiao, CHENG Li, WANG Zhi-ping (2012) "Analysis and Design for 5KW Power Factor Corrected Converter," *IEEE Power and Energy Engineering Conference (APPEEC)*.